CONCRETE LIBRARY OF JSCE NO. 24, DECEMBER 1994

# QUALITATIVE EVALUATION OF SHEAR RESISTING BEHAVIOR OF CONCRETE BEAMS REINFORCED WITH FRP RODS BY FINITE ELEMENT ANALYSIS

(Translation from Proceedings of JSCE, No.484/V-22, February 1994)

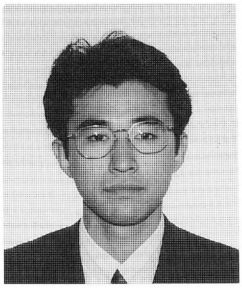
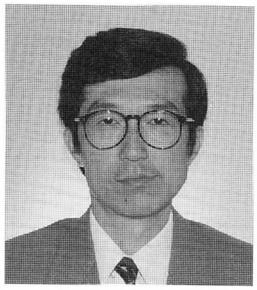
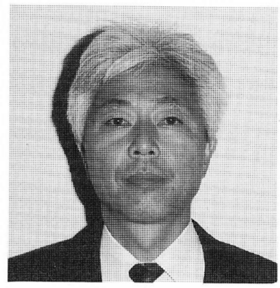

Yasuhiko SATO　　Tamon UEDA　　Yoshio KAKUTA

## SYNOPSIS

The shear resisting behavior of concrete beams reinforced with FRP rods was analytically studied by a non-linear finite element method. It was found that the analyzed results agree with experimental results with reasonable accuracy. Shear force components carried by the uncracked concrete zone and by the shear cracking zone were calculated. It was qualitatively clarified how Young's moduli of main and shear reinforcement and their yield strengths influence ultimate shear capacity of beams as well as the shear force components.

***Keywords***: *FRP rods, RC beams, shear resisting behavior, shear strength, non-linear finite element analysis*

---

Yasuhiko Sato is an assistant in the Department of Civil Engineering at Hokkaido University, Sapporo, Japan. He obtained his D.Eng. from Hokkaido University in 1994. His research interests relate to shear capacity of reinforced and prestressed concrete members. He is a member of JSCE.

Tamon Ueda is an Associate Professor in the Department of Civil Engineering at Hokkaido University. He obtained his D.Eng. from the University of Tokyo in 1982. His research interests relate to the deformation mechanism of concrete and composite structures. He is a member of JSCE.

Yoshio Kakuta is a Professor in the Department of Civil Engineering at Hokkaido University. He obtained his D.Eng. from Hokkaido University in 1968. His research interests include cracking, shear and fatigue of reinforced concrete members, partial prestressed concrete and application of continuous fiber reinforcing materials to concrete structures. He is a member of JSCE.

## 1. INTRODUCTION

Fiber reinforced plastic (FRP) rods have good properties, such as high strength, lightness, and excellent anticorrosion resistance. Therefore it is desirable to promote the use of FRP rods as reinforcement for concrete structures replacing steel bars or prestressing bars. However there are many points for careful consideration [1] when applying conventional design concept and equations to concrete structures using FRP rods. This is because FRP rod is an anisotropic material that has no yielding phenomena and a high strength but a low Young's modulus compared with steel bar.

Many reports on experimental observation of concrete members using FRP rods have been seen. As a result it has been confirmed that the shear behavior of concrete members using FRP rods is different from those using ordinary reinforcement. Tsuji et al. [2] report on beams without shear reinforcement that the shear strength of a beam reinforced with FRP rod becomes smaller than that with steel bar which has the same reinforcement ratio; and that the shear strength can be predicted by JSCE's equation [3] considering a ratio of Young's modulus of FRP rods to that of steel bar in a term of reinforcement ratio. The same results are also obtained in another experiment [4]. It can be said that the effect of FRP rod can be estimated by considering mainly the difference in Young's modulus of reinforcement.

Generally the shear force carried by shear reinforcement is calculated by a truss theory in which yielding of shear reinforcement at ultimate stage is assumed. However, in many cases a concrete beam reinforced with FRP rods fails before shear reinforcement yields. It is therefore not logical to predict that the shear strength of a concrete beam reinforced with FRP rod by a truss theory that assumes yielding of shear reinforcement. Furthermore it is possible that FRP rods at a crack intersection or bent part in a beam break before their uniaxial strength is reached [1]. At present there is no method of predicting the shear strength of concrete beams reinforced with FRP rods. It is now desirable to find an appropriate method (prediction method for shear strengths of beams reinforced with FRP rod) in order to utilize FRP rod widely in concrete structures. It is indispensable to first investigate how the mechanical properties of FRP rod used as reinforcement influence shear resisting behavior.

In this study, Young's modulus and yield strength (whether reinforcement yields or not) of main and/or shear reinforcement are chosen as analytical parameters. The aim of this study is to clarify how these mechanical properties influence shear resisting behavior in an analytical way using a non-linear finite element method. However shear failure caused by breaking of FRP rod is not considered in this study.

**Table 1** Details of Experimental Specimens

| Specimen | a/d | Concrete | Main Reinforcement | | | | Shear Reinforcement | | | |
|---|---|---|---|---|---|---|---|---|---|---|
| | | Compressive strength $f_c'$(MPa) | Material | Young's modulus $E_s$(GPa) | Tensile strength $f_{st}$(MPa) | Reinforcement ratio $p_s$(%) | Material | Young's modulus $E_w$(GPa) | Tensile strength $f_{wt}$(MPa) | Reinforcement ratio $p_w$(%) |
| NO.1 | 2.4 | 41 | aramid | 69 | 1255 | 4.08 | steel | 137 | 714 | 0.36 |
| NO.2 | 2.4 | 40 | steel | 206 | 490 | 4.77 | steel | 137 | 714 | 0.36 |
| NO.3 | 2.4 | 39 | steel | 206 | 490 | 4.77 | aramid | 69 | 1255 | 0.43 |
| NO.4 | 3.1 | 36 | steel | 206 | 368 | 4.65 | steel | 176 | 363 | 0.36 |
| NO.5 | 3.1 | 41 | steel | 206 | 368 | 4.65 | aramid | 64 | 1277 | 0.38 |

## 2. OUTLINE OF ANALYSIS

### 2.1 Finite Element Program

The non-linear finite element program used in this study was developed for shear problems of reinforced concrete beams [5]. A smeared crack model which adopts average stress and strain relationships is used in this program.

### 2.2 Definition of Failure Section and Ultimate Strength

In the analysis, ultimate strength is defined as the maximum load of a load-deflection curve. A failure section is an area where the softening of concrete is observed at the maximum load.

**Table 2** Shear Strengths

| Specimen | Test (kN) | FEM (kN) | $\frac{\text{TEST}}{\text{FEM}}$ |
|---|---|---|---|
| NO.1 | 201 | 180 | 1.11 |
| NO.2 | 262 | 244 | 1.07 |
| NO.3 | 199 | 214 | 0.93 |
| NO.4 | 170 | 186 | 0.91 |
| NO.5 | 192 | 190 | 1.01 |

## 3. EVALUATION OF EXPERIMENTAL RESULTS BY ANALYSIS

### 3.1 Experimental and Analytical Specimen

Outline of five beam specimens tested in this study are shown in Table 1 and in Fig.1. In these specimens, main and shear reinforcement ratios are almost the same in order to investigate the effect of mechanical properties of the reinforcement. Specimen NO.1 employed aramid FRP rods and specimens NO.2 to NO.5 employed steel bars as main reinforcement. Specimens NO.1 and NO.2 employed steel bars as shear reinforcement which is hardened by heating to obtain a high yield strength. Specimens NO.3 and NO.5 employed aramid FRP rod as shear reinforcement.

It is possible to consider the effect of Young's modulus of main reinforcement on shear strength by comparing shear strength of specimen NO.1 with that of specimen NO.2. It is possible to consider the effect of Young's modulus of shear reinforcement on the shear strength by comparing the shear strength of specimen NO.4 with that of specimen NO.5. In this case, the shear reinforcement of specimen NO.4 yields. The effect of the shear reinforcement yielding may be seen by comparing the shear strength of specimen NO.2 with that of specimen NO.3. In specimens NO.1 to NO.3, shear span to effective depth ratio (a/d) was fixed at 2.4. In specimens NO.4 and NO.5, a/d was fixed at 3.1. Deflections at a loading point and strains of the shear reinforcement were measured. Two-point loading was applied in the beams monotonically.

Finite element meshes are shown in Fig.2. Half of the beams was analyzed because of its symmetry. Prescribed displacements were given at the loading point directly.

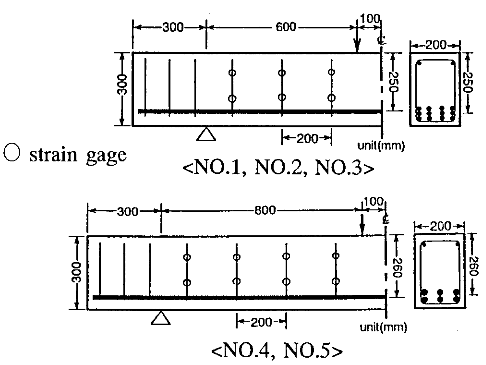


**Fig.1** Experimental Specimens

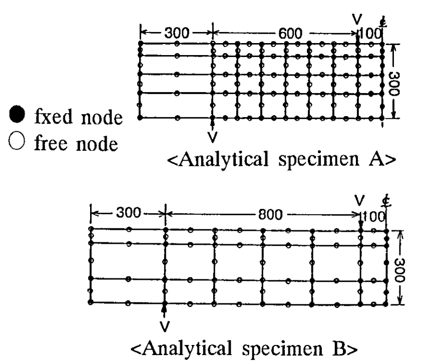


**Fig.2** Finite Element Meshes

3.2 Comparison of Experimental and Analytical Results

a ) Ultimate load

Shear compression failure occurred in all the specimens. Ultimate strengths are shown in Table 1. It is clearly seen that predicted strengths agree well with experimental ones. In both the experimental and analytical results shear strength of specimen NO.1 which has a low Young's modulus of main reinforcement is smaller by 25% than that of specimen NO.2. This indicates that a lower Young's modulus of main reinforcement gives a smaller shear strength. Shear strength of specimen NO.3 which has a low Young's modulus of shear reinforcement is smaller by 24% in the experimental results and by 12% in the analytical results than that of specimen NO.2 with a high Young's modulus which is two times of that of specimen NO.3. When Young's modulus of shear reinforcement is low, the shear strength becomes small. However the shear strength of specimen NO.5, which has a low Young's modulus but a high yield strength of shear reinforcement, is greater than that of specimen NO.4, which has a high Young's modulus but a low yield strength. This fact is also observed in the analytical results. The shear reinforcement of specimen NO.4 yields, so that the effect of the yielding appears in the shear strength.

b) Deflection

Experimental and predicted relationships between applied shear force and deflection of specimens NO.1 and NO.2 are shown in Fig.3. The predicted applied shear forces are slightly smaller than the experimental results around ultimate stage. It can be said, however, that the analysis can estimate the experimental behavior reasonably.

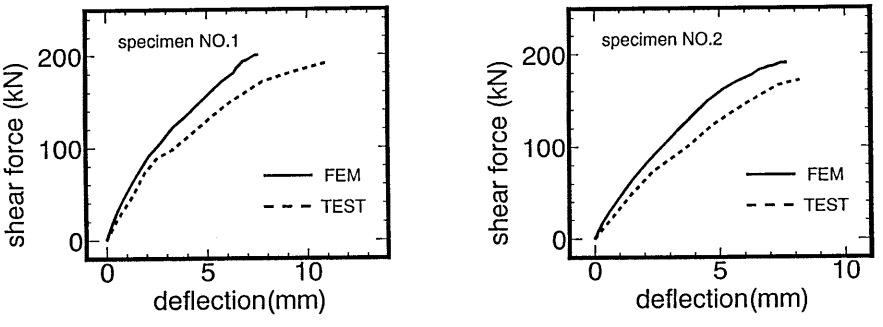


**Fig.3** Relationships between Shear Force and Deflection

c) Stress of shear reinforcement

Experimental and predicted relationships between the applied shear force and the stress of the shear reinforcement are shown in Fig.4. In the experiment, four strain gages were attached on a pair of legs of the shear reinforcement. Calculated stress is average of the measured four strains multiplied by the Young's moduli shown in Table 1. The experimental results show that for shear reinforcement with a higher Young's modulus, the tensile stress of the shear reinforcement becomes greater for the same shear force. The finite element analysis can predict this fact with sufficient accuracy.

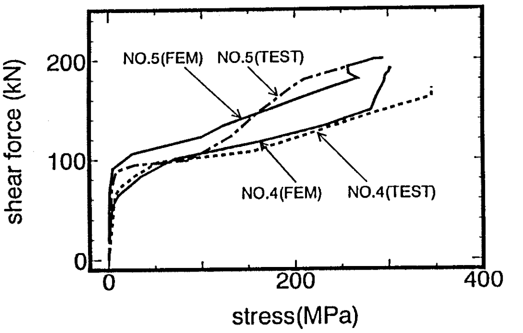


**Fig.4** Relationships between Shear Force and Stress of Shear Reinforcement

## 4. SHEAR RESISTING BEHAVIOR

4.1 Analytical Specimens

In Chapter 3, it was clarified that the shear strengths depend on the Young's modulus of the main reinforcement and the Young's modulus and the yield strength of the shear reinforcement. The finite element program can predict these dependencies of the shear strength with high accuracy. It is now analytically investigated how the mechanical properties of the reinforcement influences shear resisting behavior.
Eight specimens with the same reinforcement ratio and concrete strength were prepared in order to investigate the effect of the Young's modulus and the yield strength of the main and/or shear reinforcement. Details of the specimens, chosen with the experimental specimens in Chapter 2 in minds are shown in Table 1. Specimens PP, CP and AP contain main reinforcements with different Young's moduli, and shear reinforcements with a high yield strength. Therefore the shear reinforcement does not yield. In specimen SP, the Young's modulus of the main reinforcement is the same as that of specimen PP but the yield strength of the main reinforcement is lower than that of specimen PP. Thus the main reinforcement will yield. Specimens PP, PC and PS contain shear reinforcements with different Young's moduli. In specimen PS, the Young's modulus of the shear reinforcement is the same as that of specimen PP but the yield strength is lower than that of specimen PP, so that the shear reinforcement will yield. Specimen PP–SN has the same dimensions as specimen PP but is analyzed on the condition that a shear crack is prevented to occur. In all the specimens, a/d is fixed at 2.4 and the concrete strength is 39 MPa. Finite element mesh for the specimens is shown in Fig.2 (analytical specimen A).

**Table 3** Details of Analytical Specimens

| Analytical specimen | Concrete Compressive strength $f_c'$(MPa) | Main reinforcement Young's modulus $E_s$(GPa) | Main reinforcement Tensile strength $f_{st}$(MPa) | Shear reinforcement Young's modulus $E_w$(GPa) | Shear reinforcement Tensile strength $f_{wt}$(MPa) | Ultimate shear force V(kN) |
|---|---|---|---|---|---|---|
| AP[1) | 39 | 69 | 1255 | 206 | 1255 | 197 |
| CP | 39 | 137 | 1255 | 206 | 1255 | 235 |
| PP | 39 | 206 | 1255 | 206 | 1255 | 240 |
| SP | 39 | 206 | 343 | 206 | 1255 | 236 |
| PA | 39 | 206 | 1255 | 69 | 1255 | 225 |
| PC | 39 | 206 | 1255 | 137 | 1255 | 234 |
| PS | 39 | 206 | 1255 | 206 | 294 | 219 |
| PP-NS[2) | 39 | 206 | 1255 | 206 | 1255 | 265 |

1) AP —— shear reinforcement
└—— main reinforcement
A : Aramid P : High strength steel
C : Carbon S : Normal strength steel

2) NS : No shear cracking element

## 4.2 Components of Shear Resisting Forces

At a cracked section as shown in Fig.5, internal shear resisting forces are shear forces carried by uncracked concrete zone ($V_{ucz}$), by aggregate interlocking ($V_{agr}$), dowel action of main reinforcement ($V_{dow}$), and by shear reinforcement ($V_{web}$). Therefore shear resisting model is assumed as following.

$$V=V_{ucz}+V_{dcz}$$

where $V_{ucz}$ is the shear force carried by concrete above a tip of shear crack (uncracked zone), and $V_{dcz}$ is the shear force at shear cracking zone ($=V_{agr}+V_{dow}+V_{web}$).

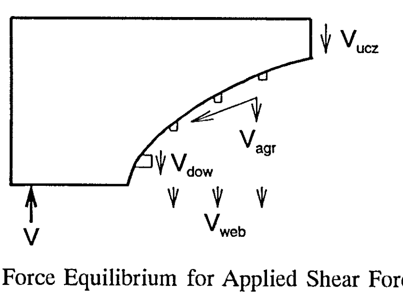


**Fig.5** Force Equilibrium for Applied Shear Force

When a shear transfer model proposed by Li and Maekawa [6] used in this study was applied for shear transfer at a crack of a RC beam, the predicted shear stress becomes slightly greater than the actual one [7]. Therefore it is assumed that this model can represent not only the shear force carried by aggregate interlocking but also the shear force by dowel action, which is not considered in the model. This model can be applied to the condition that a crack width is less than 1 mm [6].

The shear force by shear reinforcement is a tensile force sustained by reinforcement at a crack, so it is defined as a summation of average stress of the shear reinforcement and average stress of concrete.

### 4.3 Cut Plane for Consideration of Force Equilibrium

Figure 6 shows crack pattern and a cut plane for consideration of force equilibrium. Configuration of the cut plane is chosen based on the crack pattern. Because the crack patten is not the same for different Young's moduli of main and shear reinforcement, the cut planes are different for different specimens. The cut plane consists of shear crack plane and uncracked zone. The shear crack plane is defined as a path linking gauss points at which cracking occurs. The assumed shear crack plane is a plane where the shear resisting force is greatest. In the analysis shear resisting force, $V_{dcz}$, along the shear crack plane is calculated using transferred shear stress, tensile stress of concrete and reinforcement at gauss points with cracking. The shear resisting force, $V_{ucz}$ is calculated using shear stress of concrete at gauss points in the uncracked zone. The uncracked zone to calculate $V_{ucz}$ is moved in the direction parallel to member axis towards loading point (see Fig.6). These shear forces are calculated by multiplying the stresses at each gauss point by the area covered by the gauss point.

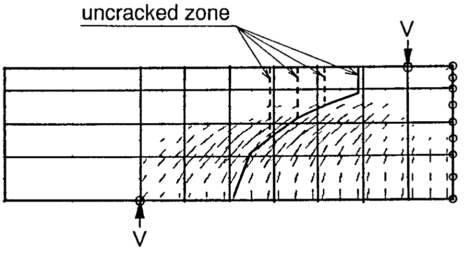


**Fig.6** Cut Plane for Consideration of Force Equilibrium

### 4.4 Effect of Young's Modulus of Main Reinforcement

The shear resisting behavior of specimens PP and AP, which contain main reinforcement with different Young's moduli, are discussed here. Figure 7 shows the variation of shear resisting forces along a cut plane with increase of applied shear force. In specimen AP with a low Young's modulus, the shear resisting force at uncracked zone, $V_{ucz}$, is smaller than that in specimen PP, while the shear resisting force at shear crack plane, $V_{dcz}$, is greater. The reason for this is that the uncracked zone of specimen AP is smaller than that of specimen PP which is caused by earlier propagation of shear crack. In specimen PP, it is observed that $V_{ucz}$ becomes smaller after the applied shear force becomes 200 kN or greater because of propagation of shear crack. Figure 8 shows the relationships between applied shear force and strain of shear reinforcement in assumed shear crack plane. It can be clearly seen that the strain of the shear reinforcement is greater in specimen AP than in specimen PP for the same applied shear force. This means that the deformation at the shear crack plane is greater. The shear resisting behavior of specimen CP with a Young's modulus of 137 GPa was between the two specimens whose Young's moduli are 206 GPa and 69 GPa. Therefore it can be said that a lower Young's modulus of main reinforcement, which causes a shear crack to propagate earlier and reduces the size of the uncracked zone, decreases the shear resisting force in the uncracked zone, $V_{ucz}$ and increases the shear resisting force, $V_{dcz}$ because of greater deformation in the shear cracking zone.

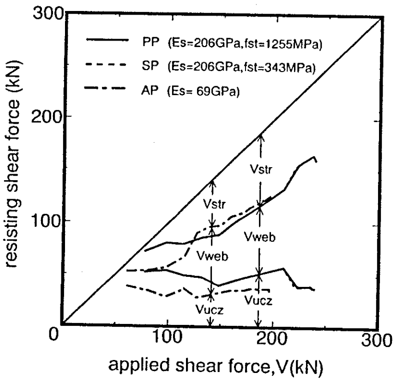


**Fig.7** Relationships between Applied Shear Force and Shear Resisting Forces (for different Young's moduli and yield strengths of main reinforcement)

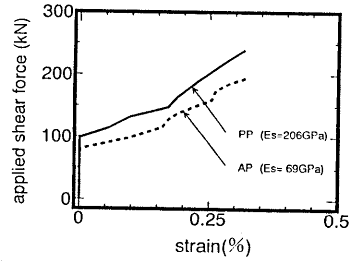


**Fig.8** Relationships between Applied Shear Force and Strain of Shear

Figure 9 shows the location of the neutral axis, which is defined by normal strain distribution, together with the tip of the shear crack. In both specimens AP and PP, the shear crack even propagates into the compression zone above the neutral axis, because the principal strain above the neutral axis is tension. The neutral axis and the shear crack tip in specimen AP are higher than those in specimen PP. The solid line in Fig.10 indicates the location of the neutral axis in the ultimate stage. The neutral axis in specimen AP is higher than that in specimen PP, so the compression zone above the neutral axis is smaller in specimen AP. The dotted line in Fig.10 indicates the neutral axis calculated by the elastic theory in which tension in the concrete is neglected. In both specimens, the location of the neutral axis calculated by the analysis are the same as that by the elastic theory in the pure-flexure region. It is observed, however, that the location of the neutral axis calculated by analysis is higher than that given by the elastic theory in the flexure-shear region.

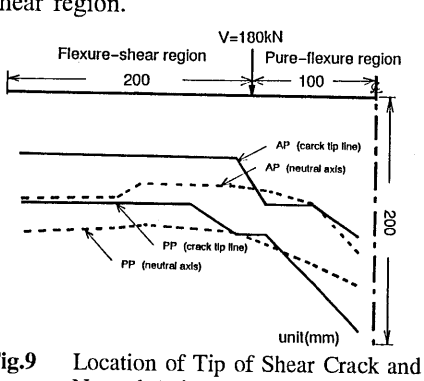


**Fig.9** Location of Tip of Shear Crack and Neutral Axis

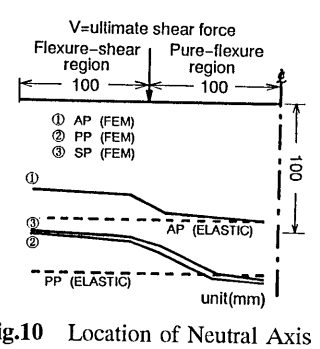


**Fig.10** Location of Neutral Axis at Ultimate Load

Figure 11 shows normal strain distributions along axes perpendicular to the member axis of specimen PP–NS, which are obtained by analysis based on the condition that shear cracking is prevented by changing the cracking criteria. The dimensions of specimen PP–NS are the same as those of specimen PP. Figure 12 shows the normal strain distributions in specimen PP. From these figures, it can be clearly seen that shear cracking moves the neutral axis upwards in the flexure–shear region, invalidating the Bernoulli–Euler hypothesis. It can be said that the size of the compression zone in the flexure–shear region decreases because of the shear cracking.

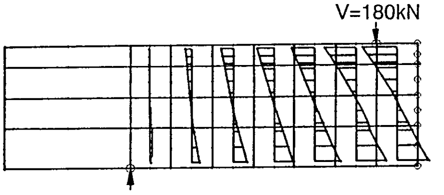


**Fig.11** Axial Normal Strain Distributions Without Shear Cracking (Specimen PP–NS)

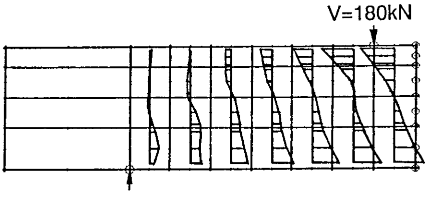


**Fig.12** Axial Normal Strain Distributions with Shear Cracking (Specimen PP)

## 4.5 Effect of Yield Strength of Main Reinforcement

The shear resisting behavior of specimens PP and SP, which contain main reinforcement with different yield strengths, are discussed here. From Fig.7 in Section 4 (4), the shear resisting force in the uncracked zone of specimen SP appears to be slightly smaller than that of specimen PP after the main reinforcement of specimen SP yields under an applied shear force of 200 kN. (In this case, the areas of the uncracked zones are the same in both cases since the locations of the shear crack tips are the same.) Figure 13 shows the relationships between the neutral axis depth at the loading point and the applied shear force. In specimen SP, the neutral axis depth decreases slightly after the main reinforcement yields. It is considered that the shear resisting force in the shear cracking zone increases and the shear resisting force in the uncracked zone decreases. However, the effect of the yielding of the main reinforcement on the shear resisting behavior cannot be clearly observed in the analytical results.

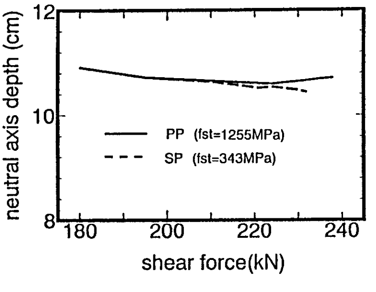


**Fig.13** Variation of Neutral Axis with Applied Shear Force

## 4.6 Effect of Young's Modulus of Shear Reinforcement

The shear resisting behavior of specimens PP and PA, which contain main reinforcement with different Young's moduli, will now be discussed. Figure 14 shows the relationships between the applied shear force and the shear resisting forces in both cases. In the case of specimen PA, in which the shear reinforcement has a low Young's modulus, after the shear force reaches at least 100 kN, the shear resisting force not due to the shear reinforcement, $V_{str}$, is observed to increase, and that due to the shear reinforcement, $V_{web}$, to decrease compared with specimen PP, in which the shear reinforcement has a high Young's modulus. Figure 15 shows the relationships between the applied shear force and the stress of the shear reinforcement in both cases. Stresses of the shear reinforcement of specimen PA, which has a low Young' modulus, are less than those of specimen PP, which has a high Young's modulus, at all the points around the ultimate stage. As shown in Fig.16, it is indicated that deformation at shear crack is greater for a less Young's modulus of shear reinforcement. If the shear resisting force due to the shear reinforcement of specimen PA were equal to that of specimen PP, the tensile strain of the shear reinforcement of specimen PA would be equal to that of specimen PP multiplied by a Young's modulus ratio ($E_{PP}/E_{PA} = 3.0$) (the dotted line in Fig.16). However the observed strains are smaller than those of given by the dotted line and then the stresses of shear reinforcement are smaller.

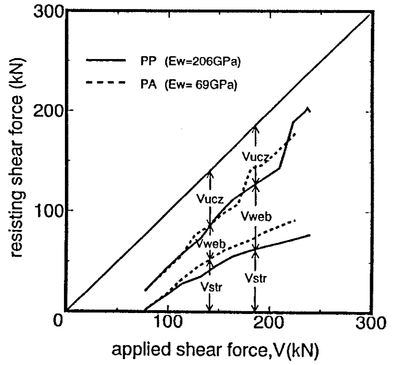


**Fig.14** Relationships between Applied Shear Force and Shear Resisting Forces (for different Young's moduli of shear reinforcement)

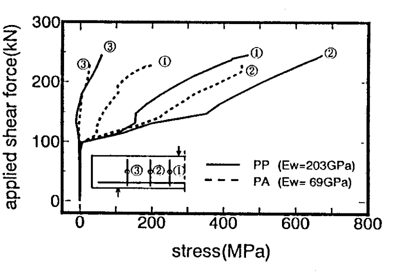


**Fig.15** Relationships between Applied Shear Force and Stress of Shear Reinforcement

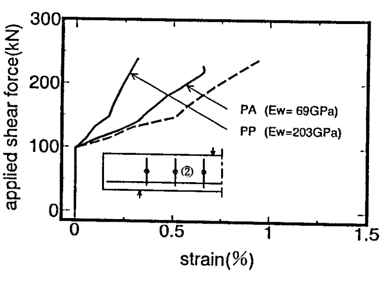


**Fig.16** Relationships between Applied Shear Force and Strain of Shear Reinforcement

Opening and sliding displacements occur at a crack. Mechanical resisting force is caused by the crack sliding. The mechanical resisting is aggregate interlocking. Figure 17 shows the relationships between the applied shear force and the ratio of shear strain to tensile strain at the middle of a shear crack. It can be clearly seen that crack sliding in specimen PA is greater than that in specimen PP, indicating that the shear stress transferred by the aggregate interlocking is greater. In the case of the shear reinforcement with a low Young's modulus, therefore, the shear resisting force due to the aggregate interlocking increases to balance the applied shear force because the shear resisting force is reduced by the shear reinforcement.

In the experimental results shown in Chapter 3, a tensile stress of the shear reinforcement which has a less Young's modulus is smaller for the same applied shear force as shown in Fig.4. Specimens NO.4 and NO.5 contain the shear reinforcement with different Young's moduli but the same reinforcement ratio. When a Young's modulus of the shear reinforcement is small, the shear resisting force by the shear reinforcement is small. The results agree well with the above mentioned analytical results.

Figure 14 indicates that shear resisting force in the uncracked zone, $V_{ucz}$ of specimen PA becomes smaller than that of specimen PP in a range of the applied shear force from 170 to 210 kN. This is caused by decrease in the area of the uncracked zone because of propagation of shear crack. Figure 18 shows that relationships between the locations of the tip of the shear crack and the neutral axis in both specimens PA and PP. It is observed that the tip of the shear crack is above the neutral axis in both cases. In the case of specimen PA with a low Young's modulus, the tip of the shear crack and the neutral axis are higher than those of specimen PP with a high Young's modulus. Figure 19 shows the neutral axis of specimens PP and PA at the ultimate stage. The neutral axis in the case of a low Young's modulus of the shear reinforcement is higher, so the size of the compression zone is smaller. It can be said that not only Young's modulus of the main reinforcement but also Young's modulus of the shear reinforcement affects the size of the compression zone. This size greatly affects the ultimate strength of a beam, as will be seen in the next chapter.

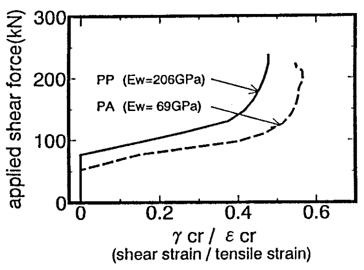


**Fig.17** Relationships between Applied Shear Force and Ratio of Shear to Tensile Strain

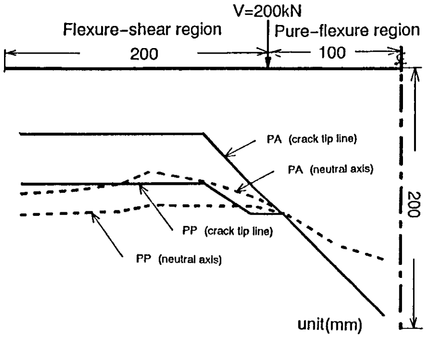


**Fig.18** Location of Tip of Shear Crack and Neutral Axis at Ultimate Load

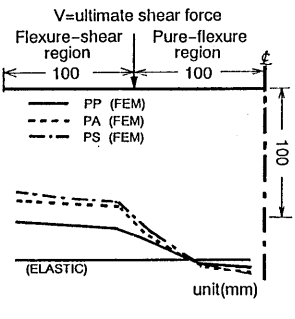


**Fig.19** Location of Neutral Axis

## 4.7 Effect of Yield Strength of Shear Reinforcement

Figure 20 shows the relationships between applied shear force and shear resisting forces for specimens PP and PS. Young's modulus of shear reinforcement in specimen PS is the same as that in specimen PP. However, its yield strength is smaller than that in specimen PP, so the shear reinforcement yields. As shown in Fig.21, which gives the relationships between applied the shear force and the stress of shear reinforcement, the shear resisting behavior of specimen PS becomes different from that of specimen PP when the applied shear force reaches 130 kN, at which yielding of the shear reinforcement occurs. If it is considered that the yielding corresponds to a reduction in Young's modulus, the shear resisting behavior would be the same as that in a beam with a low

Young's modulus. In fact, the shear resisting force by the shear reinforcement, $V_{web}$ decreases and the shear resisting force by other than shear reinforcement, $V_{str}$ increases. And shear resisting force by the uncracked concrete zone, $V_{ucz}$ of specimen PS becomes smaller than that of specimen PP around an applied shear force of 170 kN. This is caused by decreasing the size of the uncracked zone because of propagation of the shear crack.

Figure 19 in the last section also shows the neutral axes of specimens PP and PS at the ultimate strength. The location of the neutral axis of specimen PS with yielding of shear reinforcement is higher than that of specimen PP without yielding. This fact was not observed before the shear reinforcement yields. It can be considered, therefore, that the effect of yielding on the shear strength is the same as that of a low Young's modulus.

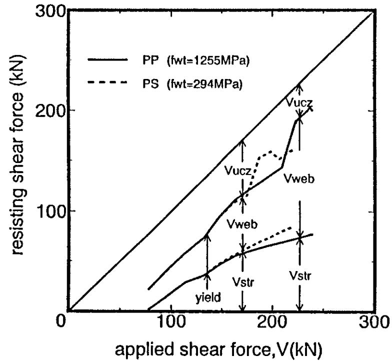


**Fig.20** Relationships between Applied Shear Force and Shear Resisting Forces (for different yield strength of shear reinforcement)

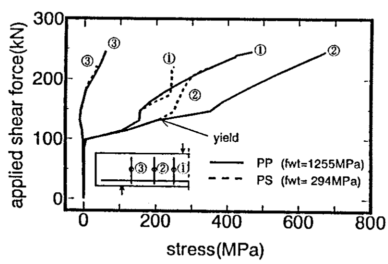


**Fig.21** Relationships between Applied Shear Force and Stress of Shear Reinforcement

## 5. SHEAR STRENGTH

### 5.1 Failure Mode

If the shear reinforcement does not yield, as seen in analytical specimens in this study, not only shear compression failure but also web concrete crushing may be anticipated. However shear strengths of the analytical specimens are much smaller than web crushing strength calculated by the JSCE equation. In the computed FEM results, softening of the concrete around the loading point is observed. It can be considered, therefore, that failure mode is the shear compression failure. Stress states of the concrete in the compression zone around the loading point are investigated in order to clarify failure criteria. Three sections, a, b, and c with respective distances of 88.7, 50.0, and 11.3 mm from the loading point are selected. The compression zone here is defined by neutral axis, which is different from $V_{ucz}$ defined in chapter 3. The shear resisting force in this compression zone is defined as $V_{cpz}$. Although the shear resisting force in shear cracking zone corresponding to $V_{cpz}$ is also different from the shear resisting force, $V_{dcz}$ defined in Chapter 3, the same symbol, $V_{dcz}$ is used.

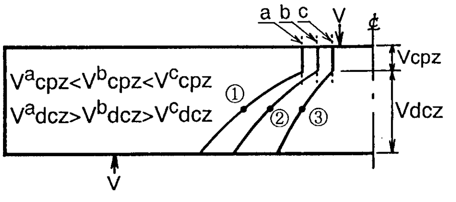


**Fig.22** Considered Cut Plane

## 5.2 Stiffness of Main Reinforcement and Failure Mechanism

Figure 23 shows the relationships between applied shear force and shear resisting force, $V_{cpz}$, in compression zone. It should be noticed that the shear resisting force increases as the distance from the loading point becomes shorter and that this tendency appears more clearly as the applied shear force becomes greater. The is because the compression zone becomes smaller as the distance from the loading point increases.

On the other hand, Fig.24 shows variation of average shear stress which is the resisting force, $V_{cpz}$, divided by area of the compression zone. For a low Young's modulus of main reinforcement (specimen PP), increment of the average stress is greater for the same applied shear force. In both specimens PP and AP, the average shear stress at section c reaches about 8 MPa when peak load is reached.

Figure 25 shows average compressive stress in the compression zone at the section c. For a low Young's modulus of main reinforcement (specimen AP), the increment of the average compressive stress is greater for the same applied shear force. The average compressive stress reaches about 30 MPa at ultimate stage. In specimen SP, in which the main reinforcement yields, a greater increment of the average compressive stress is observed after the main reinforcement yields.

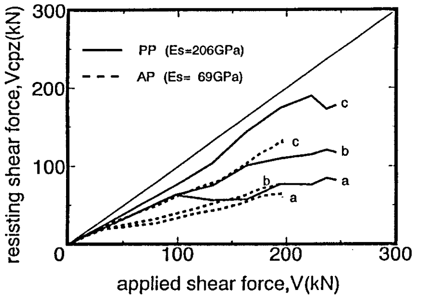


**Fig.23** Relationships between Applied Shear Force and Shear Resisting Forces in Compression Zone

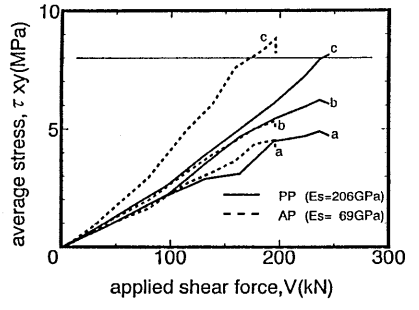


**Fig.24** Relationships between Applied Shear Force and Average Shear Stress in Compression Zone

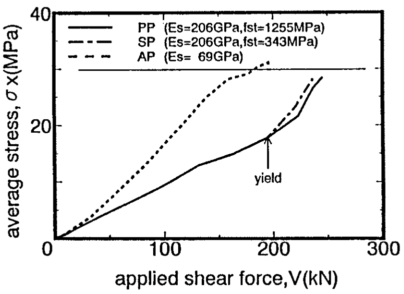


**Fig.25** Relationships between Applied Shear Force and Average Compressive Stress in Compression Zone

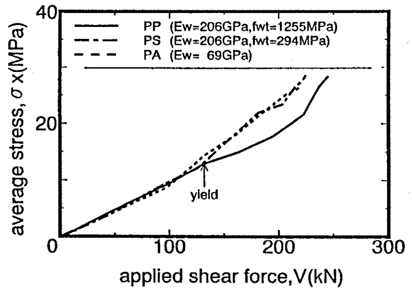


**Fig.28** Relationships between Applied Shear Force and Average Compressive Stress in Compression Zone

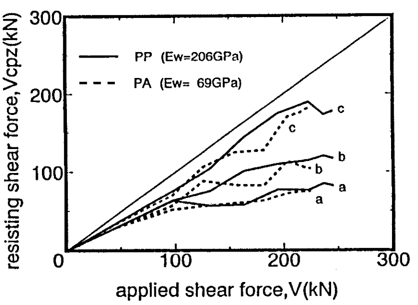


(a) for different Young's moduli of shear reinforcement

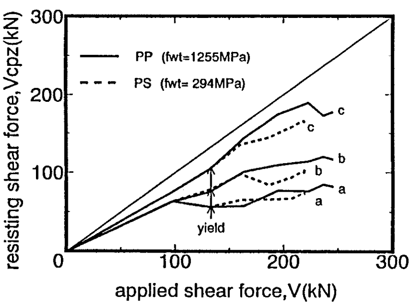


(b) for different yield strength of shear reinforcement

**Fig.26** Relationships between Applied Shear Force and Shear Resisting Force in Compression Zone

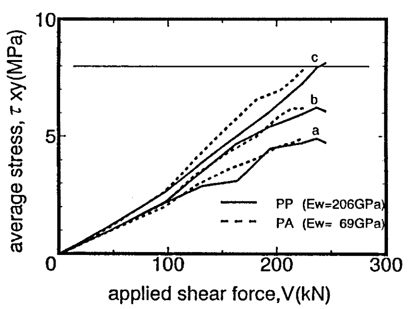


(a) for different Young's moduli of shear reinforcement

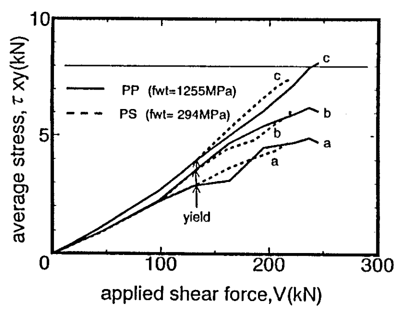


(b) for different yield strength of shear reinforcement

**Fig.27** Relationships between Applied Shear Force and Average Shear Stress in Compression Zone

## 5.3 Stiffness of Shear Reinforcement and Failure Mechanism

If the shear reinforcement has a low Young's modulus and yields, it has been found that a shear strength becomes smaller. Failure mechanism is investigated by comparing stress states in the previous three sections (see Fig.22).

Figure 26 shows the relationships between applied shear force and shear resisting force, $V_{cpz}$ in specimens PP, PA and PS. When a Young's modulus of shear reinforcement is small (specimen PA), $V_{cpz}$, is small at each section. In the case of specimen PS, in which the shear reinforcement yields, it is observed that $V_{cpz}$ becomes smaller after the shear reinforcement yields. This is because the size of the compression zone decreases in the cases of a low Young's modulus and yielding of shear reinforcement.

Figure 27 shows the variation of average shear stress at each section. The rate of increase of the average stress at the section c of specimen PA with a low Young's modulus is greater than that of specimen PP with a high Young's modulus of shear reinforcement (see Fig.27(a)). A greater increment of the average shear stress is also found in specimen PP after yielding of the shear reinforcement, as shown in Fig.27(b). In each specimen, peak load is observed when the average stress at the section c reaches about 8 MPa. On the other hand, Fig.28 shows variation of average compressive stress at the section c. When Young's modulus of the shear reinforcement is small (specimen PA), the rate of increase of the average compressive stress is great. The average stresses in specimens PP and PA reach about 30 MPa at the ultimate stage. In the case of specimen PS, in which the shear reinforcement yields, the same tendency is observed.

## 5.4 Evaluation of Shear Strength

It was investigated in Sections 5 (2) and (3) how Young's modulus and the yield strength of main and shear reinforcement influence stress states in the compression zone. It was found that the analytical specimens failed when the average stresses reached about the same level, namely the average shear stress of 8 MPa and the average compressive stress of 30 MPa. (See Table 4.) The maximum compressive stress was about 1.2 times as great as uniaxial concrete strength and softening of concrete was observed after the stress reached the maximum value. The concrete stresses become greater than the uniaxial strength because the compression zone in the section c is under biaxial compression [8]. If these average stresses at failure were the critical stresses for the analytical specimens, it could be said that the shear strength of a specimen in which main and/or shear reinforcement has a low Young's modulus becomes smaller because small compression zone causes greater increment of stresses in the zone. If the shear reinforcement has a low yield strength and yields, the same can be said.

The critical stresses are important factors in predicting the shear strength. A numerical analysis with a wide range of parameters, such as a/d and concrete strength, is necessary in order to quantify the critical stresses.

**Table 4** Maximum and Average Stresses in Compression Zone at Ultimate Load

| Specimen | Maximum | | Average | |
|---|---|---|---|---|
| | $\sigma_x$ (MPa) | $\tau_{xy}$ (MPa) | $\sigma_x$ (MPa) | $\tau_{xy}$ (MPa) |
| AP | 47.0 | 15.0 | 28.7 | 8.8 |
| CP | 46.5 | 13.3 | 30.1 | 7.8 |
| PP | 45.8 | 12.3 | 28.5 | 8.2 |
| SP | 45.8 | 13.1 | 28.2 | 8.1 |
| PA | 46.5 | 12.7 | 28.6 | 7.9 |
| PC | 45.8 | 12.0 | 28.9 | 7.7 |
| PS | 45.8 | 12.1 | 27.8 | 7.4 |

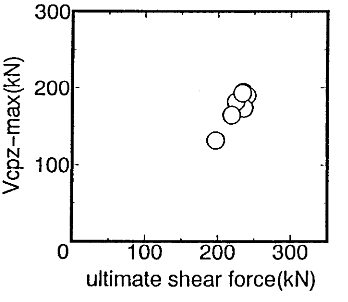


**Fig.29** Relationships between Ultimate Shear Strength and Shear Resisting Force in Compression Zone

Figure 29 shows the relationships between the ultimate shear strength and the maximum value of the shear resisting force, $V_{cpz}$ at the section c. It can be clearly seen that the maximum of shear resisting force increases as the ultimate strength increases. Development of a calculation method for the critical stresses and size of the compression zone is necessary to predict the shear strength. The size of the compression zone is affected by Young's modulus of the main and/or shear reinforcement. If the relationships between shear resisting force in the compression zone and shear resisting force in the shear cracking zone can be uniquely determined, the shear strength can be predicted by simple calculation.

## 5.5 Stiffness of Reinforcement and Shear Strength

From the experimental results, it was ascertained that the shear strengths depend on the mechanical properties of reinforcement. It was confirmed that the dependency of the shear strengths could be predicted with good accuracy by the FEM. The relationships between the stiffness of the shear reinforcement and shear strength of the seven specimens in this study is summarized in Fig.30. The vertical axis indicates the shear strength ($V_u$) and the horizontal axis indicates Young's modulus of shear reinforcement ($E_w$). Solid lines are $V_u$–$E_w$ relationships for different Young's moduli of main reinforcement where the shear reinforcement does not yield. Subscripts A, C, and S of symbol E indicate aramid FRP rod, carbon FRP rod and steel bar respectively.

When the yielding strength of shear reinforcement is high enough, the shear strength increases as the Young's modulus of main reinforcement increases ($V_{uPP} > V_{uCP} > V_{uAP}$). Furthermore the shear strength increases as Young's modulus of shear reinforcement increases ($V_{uPP} > V_{uPC} > V_{uPA}$). If the shear reinforcement yields, however, the shear strength becomes smaller than that of a specimen in which shear reinforcement does not yield ($V_{uPP} > V_{uPS}$). It is also possible that the shear strength of a specimen with a low Young's modulus is greater than that of a specimen with a high Young's modulus but a low yield strength ($V_{uPC} > V_{uPA} > V_{uPS}$).

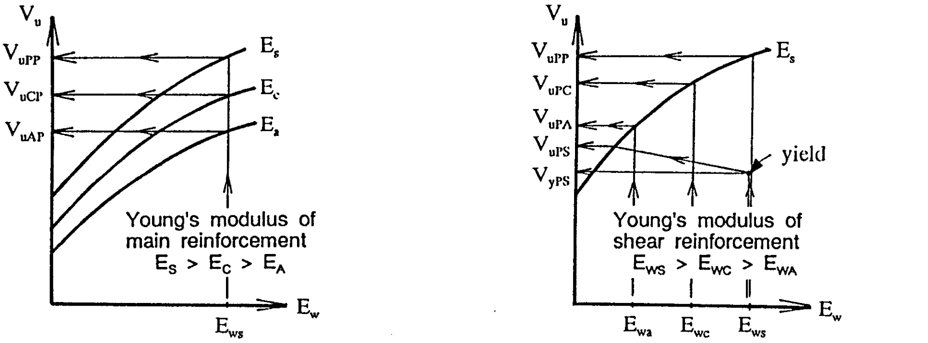


(a) for different Young's moduli of main reinforcement (b) for different Young's moduli of shear reinforcement

**Fig.30** Stiffness of Reinforcement and Shear Strength

## 6. CONCLUSIONS

In this study the following conclusions are obtained.

(1) Non–linear finite element analysis can predict the ultimate strength, deformational behavior, and stress of reinforcement with reasonable accuracy.

(2) Finite element analysis indicates that the Bernoulli–Euler hypothesis is not applicable and neutral axis depth becomes small in flexure–shear region after shear cracking has occurred. It is clarified that the neutral axis depth becomes smaller as Young's modulus of main and/or shear reinforcement becomes smaller. It is also indicated that yielding of shear reinforcement reduces the neutral axis depth.

(3) When Young's modulus of main reinforcement is low, the shear resisting force in an uncracked zone is small, but the shear resisting force along the shear crack plane is large.

(4) When Young's modulus of shear reinforcement is low, the shear resisting force in an uncracked zone is small, but the shear resisting force along the shear crack plane is large, as seen when Young's modulus of main reinforcement is low. The shear resisting force at shear crack plane consist of shear resisting forces by shear reinforcement and by other than shear reinforcement. When Young's modulus is low, the latter becomes larger.

(5) Analytical specimens in which a/d equals 2.4 and concrete strength is 30 MPa fail when the average shear and compressive stresses in a compression zone in flexure–shear region reach certain values. It is indicated that if the average stresses were the critical stresses for the analytical specimens, it could be said that a shear strength of a specimen in which main or shear reinforcement has a low Young's modulus becomes small because compression zone whose size is reduced by the low Young's modulus causes high stresses in the zone. When shear reinforcement has a high Young's modulus but yields, the same phenomena is observed.

(6) As Young's modulus of main or shear reinforcement decreases, the shear strength decreases. When shear reinforcement yields, the shear strength becomes smaller than that of a specimen in which shear reinforcement does not yield. The shear strength of a specimen which has shear reinforcement with a low Young's modulus can be greater than that of a specimen which has shear reinforcement with a high Young's modulus but a low yield strength.

## Notations

$V$ : Applied shear force
$V_{ucz}$ : Shear resisting force carried by uncracked concrete
$V_{cpz}$ : Shear resisting force carried by concrete above neutral axis (compression zone)
$V_{dcz}$ : Shear resisting force along shear crack plane
$V_{web}$ : Shear resisting force carried by shear reinforcement
$V_{str}$ : Shear resisting force carried by means other than shear reinforcement ( $V_{str} = V_{agr} + V_{dow}$)
$V_{agr}$ : Shear resisting force carried by aggregate interlocking
$V_{dow}$ : Shear resisting force carried by dowel action

## Acknowledgements

We would like to thank Dr. Nares Pantaratorn, who developed the finite element program used in this study, Mr. Tsutomu Kimura for his assistance in experimental work, and Mitsui Co., Ltd., for providing material. This research was partly supported by the Grant–in Aid for Scientific Research 1992, Ministry of Education, Science and Culture of Japan (Grant No. 04302040, Principal Investigator: Prof. Yoshio Kakuta, Hokkaido University) and the Research Scholarship of the Yoshida Prize of the JSCE in 1991.

## References

[1] JSCE Subcommittee for Studies on Continuous Fiber, "Present State of Technology Concerning Application to the Field of Civil Engineering Structures of Concrete–Base Composite Material Using Continuous Fiber", 1992 (in Japanese)
[2]Tsuji, Y., Saito, H., Sekijima, K., and Ogawa, H., "Flexural and Shear Behaviors of Concrete Beams Reinforced with FRP Rods", Proc. of JCI, Vol.10, No.3, pp. 547–552, 1988 (in Japanese)
[3] JSCE, "Standard Specification for Design and Construction of Concrete Structures", 1986
[4]Amano, R., Murayama, Y., Okumura, K., and Bujadaham, B., "Shear Property of Beams Reinforced with FRP Rods as Tensile Reinforcement", Proc. of JSCE Symposium on Concerning Application to the Field of Civil Engineering Structures of Concrete–Based Composite Material Using Continuous Fibers", pp. 181–186, 1992 (in Japanese)

[5] Pantaratorn, N., "Finite Element Analysis on Shear Resisting Mechanism of RC Beams", Dissertation Submitted to the University of Tokyo, 1991
[6] Li, B., Maekawa, K., and Okamura, H., "Contact Density Model for Stress Transfer Across Cracks in Concrete", Journal of the Faculty of Engineering, University of Tokyo (B), Vol.40, No.1, pp. 9–52, 1989
[7] Pantaratorn, N. and Ueda, T., "Analysis of Beams with Shear Reinforcement by Finite Element Method", Proc. of JCI, Vol.13, No.2, pp. 1021–1026, 1991
[8] Maekawa, K. and Okamura, H., "The Deformational Behavior and Constitutive Equation of Concrete Using Elasto-plastic and Fracture Model", Journal of the Faculty of Engineering, University of Tokyo (B), Vol.37, No.2, pp. 253–328, 1983